Synthesis, Spectroscopy, and Structural Studies of Tetrakis(*O*-alkyl dithiocarbonato)germanium. Crystal Structures of $Ge[S_2COR]_4$, Where R = Me, Et, and *i*-Pr

John E. Drake,* Anil G. Mislankar, and Jincai Yang

Department of Chemistry and Biochemistry, University of Windsor, Windsor, Ontario, Canada N9B 3P4

Received April 27, 1992

The tetrakis(*O*-alkyl dithiocarbonato)germanium derivatives $Ge[S_2COMe]_4$, $Ge[S_2COEt]_4$, and $Ge[S_2CO(i\text{-}Pr)]_4$ have been prepared in 55–65% yields by reaction of the sodium salt of the dithiocarbonic (xanthic) acid with tetrachlorogermane. The compounds were characterized by infrared, Raman, and ^1H and ^{13}C NMR spectroscopy. The crystal structures of all three compounds were determined. $Ge[S_2COMe]_4$ (**1**), which crystallizes as orthorhombic in space group $I4_1/a$ (No. 88), has the cell parameters a = 16.831 (2) Å, b = 16.831 (2) Å, c = 6.6598 (6) Å, V = 1887 (1) Å^3, Z = 4, R = 0.0384, and R_w = 0.0408. The environment about germanium is essentially that of a distorted tetrahedron with monodentate xanthate ligands resulting in two S–Ge–S angles of 92.4 (1)° and four of 118.62 (7)°. $Ge[S_2COEt]_4 \cdot CS_2$ (**2**), which also crystallizes as orthorhombic ($I4_1/a$, No. 88), has the cell parameters a = 14.659 (7) Å, b = 14.659 (7) Å, c = 12.371 (5) Å, V = 2659 (2) Å^3, Z = 4, R = 0.0400, and R_w = 0.0386. In this case, the distorted tetrahedron results in four smaller S–Ge–S angles of 106.88 (5)° and two larger ones of 114.8 (1)°. $Ge[S_2CO(i\text{-}Pr)]_4$ (**3**), which crystallizes as triclinic in space group $P\bar{1}$ (No. 2), has the cell parameters a = 8.366 (1) Å, b = 11.761 (1) Å, c = 15.285 (3) Å, α = 90.62 (1)°, β = 93.60 (1)°, γ = 109.40 (1)°, V = 1415 (1) Å^3, Z = 2, R = 0.0500, and R_w = 0.0520. The distortion is similar to that observed in **2** with the average of the four smaller S–Ge–S angles being 105 (1)° and that of the two larger ones being 119.6 (7)°. The Ge–S bond distances of 2.200 (2) Å in **1** are shorter than in **2** or **3** where the distances are 2.238 (2) Å and an average of 2.237 (4) Å, respectively. In the three compounds, the Ge---O nonbonding distances range from 2.932 (4) to 2.971 (5) Å while the Ge---S nonbonding distances range from 4.639 (2) to 4.749 (2) Å. Attempts to isolate mixed chloro(xanthate) species such as $ClGe[S_2COR]_3$, $Cl_2Ge[S_2COR]_2$, and $Cl_3Ge[S_2COR]$ were not successful.

Introduction

We recently confirmed that the xanthate ligands in a variety of xanthate derivatives of mono-, di-, and triphenylgermane are all oriented with the oxygen atom rather than with the second sulfur atom in the nonbonding position nearest the metal.[1,2] While this is also true for bis(*O*-ethyl xanthato)bis(quinolin-8-olato)-tin(IV),[3] it is not true for the xanthate groups in tetrakis[diethyl xanthato)tin or $Sn(S_2COEt)_2Br_2$, where bidentate linkages have been reported.[4] We therefore attempted to form a series of substituted chloro derivatives of germanium, culminating in the fully substituted species. However, despite attempts to make and isolate all of the following species, $Cl_3Ge[S_2COR]$, $Cl_2Ge[S_2CO_2R]_2$, $ClGe[S_2COR]_3$, and $Ge[S_2COR]_4$, where R = Me, Et, *i*-Pr, only the tetrakis compounds were successfully separated, characterized by ^1H and ^{13}C NMR spectroscopy, infrared and Raman spectroscopy, and single-crystal X-ray crystallography.

Experimental Section

Materials. Tetrachlorogermane was obtained from Gelest Inc. and used as supplied. Potassium *O*-methyl dithiocarbonate, *O*-ethyl dithiocarbonate, and *O*-isopropyl dithiocarbonate were prepared by adding a slight excess of CS_2 into a mixture of equimolar amounts of KOH and ROH (where R = Me, Et, *i*-Pr) in the manner described previously,[5] and their purity was checked by ^1H and ^{13}C NMR spectroscopy. Distilled carbon disulfide (dried over P_4O_{10}) was used as the solvent in all reactions. The reactions were carried out on a vacuum line to exclude air and moisture.

Preparation of Tetrakis(*O*-organyl dithiocarbonato)germanium(IV) Compounds. Typically, degassed tetrachlorogermane (0.2 mL, 1.75 mmol) and CS_2 (approximately 8 mL) were distilled onto the previously dried and degassed potassium *O*-organyldithiocarbonate (approximately 8 mmol to ensure more than 4-fold excess) at −196 °C. The liquid nitrogen trap was removed and the contents allowed to warm to ambient temperature with stirring which was then continued for 5 h. The mixture was then filtered to remove KCl and the solvent evaporated. The yellow solid product was redissolved in CS_2 and kept in the refrigerator. Yellowish crystals appeared after 3–5 days. Thus were formed $Ge[S_2COMe]_4$ (**1**): needle-shaped yellow crystals; yield 65%, mp 107–108 °C. $Ge[S_2COEt]_4 \cdot CS_2$ (**2**): needle-shaped yellow crystals; yield 55%; mp 75–77 °C. $Ge[S_2CO(i\text{-}Pr)]_4$ (**3**): block-shaped yellow crystals; yield 60%; mp 126–127 °C.

Attempted Preparation of Mono-, Bis-, and Tris-Substituted Derivatives. Typically, degassed tetrachlorogermane (0.2 mL, 1.75 mmol) and CS_2 (approximately 8 mL) were distilled onto the previously dried and degassed potassium *O*-organyldithiocarbonate in equimolar (1.75 mmol), 2-fold excess (3.50 mmol) or 3-fold excess (5.25 mmol) amounts. The workup was performed in each case as described for the formation of the tetrakis compounds. However, in all cases a viscous yellow oil resulted and in no case was it possible to isolate crystalline compounds. In all cases, the NMR spectra of the CS_2 solution prior to workup were consistent with the presence of at least three dithiocarbonate derivatives and were similar in appearance regardless of the initial ratio of reactants.

Physical Measurements. Density measurements were performed by the flotation method. The ^1H and ^{13}C NMR spectra were recorded on a Bruker 300 FT/NMR spectrometer in $CDCl_3$ or CS_2. The infrared spectra were recorded on a Nicolet 5DX FT spectrometer as CsI pellets. The Raman spectra were recorded on a Spectra-Physics 164 spectrometer using the 5145-Å exciting line of an argon ion laser with samples sealed in capillary tubes. The melting points were determined on a Fisher-Johns apparatus.

X-ray Crystallographic Analysis. Needlelike crystals of **1** and **2** and blocklike crystals of **3** were sealed in thin-walled glass capillaries and mounted on a Rigaku AFC6S diffractometer, with graphite-monochromated Mo Kα radiation.

Cell constants and an orientation matrix for data collection, obtained from a least-squares refinement using the setting angles of 25 carefully centered reflections in the range $20 < 2\theta < 26°$ and $34 < 2\theta < 38°$, corresponded to tetragonal (for **1** and **2**) and to triclinic (for **3**) cells, the dimensions being given in Table I. On the basis of the systematic absences

(1) Drake, J. E.; Sarkar, A. B.; Wong, M. L. Y. *Inorg. Chem.* **1990**, *29*, 785.
(2) Drake, J. E.; Mislankar, A. G.; Wong, M. L. Y. *Inorg. Chem.* **1991**, *30*, 2174.
(3) Raston, C. L.; White, A. H.; Winter, G. *Aust. J. Chem.* **1978**, *31*, 2641.
(4) Gable, R. W.; Raston, C. L.; Rowbottom, G. L.; White, A. H.; Winter, G. *J. Chem. Soc., Dalton Trans.* **1981**, 1392. Raston, C. L.; Tennant, P. R.; White, A. H.; Winter, G. *Aust. J. Chem.* **1978**, *31*, 1493.
(5) Vogel, A. I. *Practical Organic Chemistry*; Longmans: New York, 1956; p 499.

0020-1669/92/1331-5543$03.00/0

Table I. Crystallographic Data for $Ge[S_2COMe]_4$ (**1**), $Ge[S_2COEt]_4 \cdot CS_2$ (**2**), and $Ge[S_2CO(i\text{-}Pr)]_4$ (**3**)

	$Ge[S_2COMe]_4$ (1)	$Ge[S_2COEt]_4 \cdot CS_2$ (2)	$Ge[S_2CO(i\text{-}Pr)]_4$ (3)
chem formula	$C_8H_{12}O_4S_8Ge$	$C_{13}H_{20}O_4S_{10}Ge$	$C_{16}H_{28}O_4S_8Ge$
fw	501.25	633.49	613.46
a, Å	16.831 (2)	14.659 (7)	8.366 (1)
b, Å	16.831 (2)	14.659 (7)	11.761 (1)
c, Å	6.6598 (6)	12.371 (5)	15.285 (3)
α, deg	90.00	90.00	90.62 (1)
β, deg	90.00	90.00	93.60 (1)
γ, deg	90.0	90.00	109.40 (1)
V, Å^3	1887 (1)	2659 (2)	1415 (1)
space group	$I4_1/a$	$I4_1/a$	$P\bar{1}$
Z	4	4	2
T, °C	23	−40	23
λ, Å	0.710 69	0.710 69	0.710 69
ρ_{obsd}, g cm^{-3}	1.76	1.55	1.40
ρ_{calcd}, g cm^{-3}	1.81	1.58	1.44
μ, cm^{-1}	24.60	19.08	16.50
transm factors	0.86–1.00	0.93–1.00	0.61–1.00
R	0.0384	0.0400	0.0500
R_w	0.0408	0.0386	0.0520

of hkl ($h + k + l \neq 2n$), $hk0$ ($h \neq 2n$) and $00l$ ($l \neq 4n$), packing considerations, statistical analysis and successful solution and refinement of the structure, the space groups for **1** and **2** were determined to be $I4_1/a$ (No. 88). For compound **3**, the space group was determined to be $P\bar{1}$ (No. 2).

The data were collected at a temperature of 23 ± 1 °C for **1** and **3** and −40 ± 1 °C for **2** by using the ω–2θ scan technique to a maximum 2θ value of 50.0°. The ω scans of several intense reflections, made prior to data collection, had an average width at half-height of 0.33° (for **1**), 0.30° (for **2**), and 0.29° (for **3**) with a takeoff angle of 6.0°. Scans of (1.63 + 0.30 tan θ)° for **1**, (1.21 + 0.30 tan θ)° for **2**, and (1.50 + 0.30 tan θ)° for **3**, were made at a speed of 32.0°/min (in ω). The weak reflections ($I < 10.0\sigma(I)$) were rescanned (maximum of two rescans), and the counts were accumulated to assure good counting statistics. Stationary background counts were recorded on each side of the reflection. The ratio of peak counting time to background counting time was 2:1. The diameter of the incident beam collimator was 0.5 mm, and the crystal to detector distance was 250.0 mm (for **1** and **2**) and 400.0 mm (for **3**).

Of the 753 (for **1**), 1346 (for **2**), or 5352 (for **3**) reflections which were collected, 633 (for **1**), 1244 (for **2**), or 4974 (for **3**) were unique (R = 0.122 (for **1**), 0.051 (for **2**), or 0.288 (for **3**)). The intensities of three representative reflections which were measured after every 150 reflections declined by 46% for **1**, and consequently, a linear correction factor was applied to the data to account for this phenomenon. Decay of **2** was greater than 50%, and as a result it was not possible to collect reliable data at room temperature. However, by utilizing recently acquired low-temperature facilities, the data on **2** were re-collected at −40 °C with no decay occurring. Surprisingly, there was no significant decay during the data collection of **3**.

The linear absorption coefficient for Mo Kα is 24.6 cm^{-1} for **1**, 19.1 cm^{-1} for **2**, and 16.5 cm^{-1} for **3**. An empirical absorption correction, based on azimuthal scans of several reflections, was applied, which resulted in transmission factors ranging from 0.86 to 1.00 (for **1**), 0.93 to 1.00 (for **2**), and 0.61 to 1.00 (for **3**). The data were corrected for Lorentz and polarization effects.

The structures were solved by direct methods.[6] The non-hydrogen atoms, other than the carbon atoms in **1** where the data was limited, were refined anisotropically. The hydrogen atoms were included in their idealized positions with C–H set at 0.95 Å and with isotropic thermal parameters set at 1.2 times that of the carbon atom to which they were attached. The final cycles of full-matrix least-squares refinement[7] were based on 308 (for **1**), 588 (for **2**), and 2804 (for **3**) observed reflections ($I > 3.00\sigma(I)$) and 38 (for **1**), 64 (for **2**), and 262 (for **3**) variable parameters and converged (largest parameter shifts were 0.0008 (for **1** and **2**) and 0.003 (for **3**) times its esd) with unweighted and weighted agreement factors of $R = \sum||F_o| - |F_c||/\sum|F_o| = 0.0384$ for **1**, 0.0400 for **2**, and 0.0500 for **3** and $R_w = [(\sum w(|F_o| - |F_c|)^2/\sum wF_o^2)]^{1/2} = 0.0408$ for **1**, 0.0386 for **2**, and 0.0520 for **3**.

The standard deviation of an observation of unit weight[8] was 1.50 (for **1**), 1.05 (for **2**), and 1.62 (for **3**). The weighting scheme was based on counting statistics and included a factor ($p = 0.03$) to downweight the intense reflections. Plots of $\sum w(|F_o| - |F_c|)^2$ versus $|F_o|$, reflection order in data collection, (sin θ)/λ, and various classes of indices showed no unusual trends. The maximum and minimum peaks on the final difference Fourier map corresponded to +0.31 and −0.26 for **1**, +0.32 and −0.33 for **2**, and +0.78 and −0.83 e/Å^3 for **3**.

Neutral-atom scattering factors were taken from Cromer and Waber.[9] Anomalous dispersion effects were included in F_c;[10] the values for $\Delta f'$ and $\Delta f''$ were those of Cromer.[11] All calculations were performed using the TEXSAN[12] crystallographic software package of Molecular Structure Corp.

The final atomic coordinates and equivalent isotropic thermal parameters for the non-hydrogen atoms are given in Tables II–IV, important distances and bond angles in Tables V–VII, and ORTEP diagrams of **1**–**3** in Figures 1–3, respectively. Additional crystallographic data are available as supplementary material.

Table II. Final Fractional Coordinates and B(eq) for Non-Hydrogen Atoms of $Ge[S_2COMe]_4$ (**1**) with Standard Deviations in Parentheses

atom	x	y	z	B(eq), Å^2
Ge	0	1/4	1/8	3.28 (5)
S(1)	0.0417 (1)	0.3347 (1)	−0.1036 (3)	4.4 (1)
S(2)	0.0114 (2)	0.4856 (1)	−0.0916 (4)	5.2 (1)
O(1)	0.0661 (3)	0.4074 (3)	0.2220 (8)	4.0 (3)
C(1)	0.0764 (4)	0.4143 (5)	0.027 (1)	2.9 (2)
C(2)	0.0919 (5)	0.4699 (6)	0.350 (1)	5.6 (2)

Table III. Final Fractional Coordinates and B(eq) for Non-Hydrogen Atoms of $Ge[S_2COEt]_4 \cdot CS_2$ (**2**) with Standard Deviations in Parentheses

atom	x	y	z	B(eq), Å^2
Ge	0	1/4	1/8	2.17 (4)
S(1)	−0.1266 (1)	0.2725 (1)	0.2225 (1)	3.15 (9)
S(2)	−0.1768 (1)	0.4114 (1)	0.3808 (2)	5.2 (1)
O(1)	−0.0182 (3)	0.4007 (3)	0.2793 (4)	3.2 (2)
C(1)	−0.1014 (5)	0.3699 (4)	0.2996 (6)	3.1 (3)
C(2)	0.0139 (6)	0.4821 (5)	0.3359 (6)	5.0 (5)
C(3)	0.1030 (6)	0.5045 (6)	0.2922 (9)	7.8 (6)
S(3)	0	1/4	0.5037 (3)	9.8 (3)
C(4)	0	1/4	5/8	4.5 (5)

Results and Discussion

The three tetrakis compounds were prepared in 55–65% yield by the addition of a slight excess of the potassium salt to a carbon disulfide solution of tetrachlorogermane in accord with the simple equation

$$GeCl_4 + 4KS_2COR \rightarrow Ge[S_2COR]_4 + 4KCl$$

$$R = Me, Et, i\text{-}Pr$$

All three compounds could be recrystallized from carbon disulfide to give X-ray-quality crystals. However, they decomposed rapidly when separated from the supernatant liquid to the

(6) Structure solution methods: Calbrese, J. C. PHASE—Patterson Heavy Atom Solution Extractor. Ph.D. Thesis, University of Wisconsin—Madison, 1972. Beurskens, P. T. DIRDIF: Direct Methods for Difference Structures—an automatic procedure for phase extension and refinement of difference structure factors. Technical Report 1984/1; Crystallography Laboratory: Toernooiveld, 6525 Ed Nijmedgen, Netherlands, 1984.

(7) Least squares: Function minimized $\sum w(|F_o| - |F_d|)^2$, where $w = 4F_o^2(F_o^2)$, $\sigma^2(F_o^2) = [S^2(C + R^2B) + (pF_o^2)^2]/(Lp)^2$, S = scan rate, C = total integrated peak count, R = ratio of scan time to background counting time, B = total background count, Lp = Lorentz–polarization factor, and p = p factor.

(8) Standard deviation of an observation of unit weight: $[\sum w(|F_o| - |F_d|)^2/N_o - N_v)]^{1/2}$, where N_o = number of observations and N_v = number of variables.

(9) Cromer, D. T.; Waber, J. T. *International Tables for X-ray Crystallography*; The Kynoch Press: Birmingham, England, 1974; Vol. IV, Table 2.2 A.

(10) Ibers, J. A.; Hamilton, W. C. *Acta Crystallogr.* **1964**, *17*, 781.

(11) Cromer, D. T. *International Tables for X-ray Crystallography*; The Kynoch Press: Birmingham, England, 1974; Vol. IV, Table 2.3.1.

(12) *TEXSAN-TEXRAY Structure Analysis Package*; Molecular Structure Corp.: Weedlands, TX, 1985.

Table IV. Final Fractional Coordinates and B(eq) for Non-Hydrogen Atoms of $Ge[S_2CO(i\text{-}Pr)]_4$ (**3**) with Standard Deviations in Parentheses

atom	x	y	z	B(eq), Å^2
Ge	0.9892 (1)	0.16398 (7)	0.74901 (5)	3.15 (3)
S(1)	1.1617 (2)	0.1061 (2)	0.6670 (1)	3.79 (8)
S(2)	1.1178 (3)	-0.1103 (2)	0.5609 (1)	4.9 (1)
S(3)	0.8118 (2)	0.2164 (2)	0.6547 (1)	4.16 (8)
S(4)	0.5876 (3)	0.3563 (2)	0.6717 (2)	5.8 (1)
S(5)	1.1657 (2)	0.3014 (2)	0.8445 (1)	4.20 (8)
S(6)	1.3821 (3)	0.5511 (2)	0.8293 (1)	5.1 (1)
S(7)	0.8138 (2)	0.0286 (2)	0.8316 (1)	4.48 (9)
S(8)	0.8448 (4)	-0.1681 (2)	0.9374 (2)	6.8 (1)
O(1)	0.8692 (6)	-0.0549 (4)	0.6320 (3)	4.1 (2)
O(2)	0.7729 (6)	0.3042 (4)	0.8028 (3)	4.3 (2)
O(3)	1.1980 (6)	0.4070 (4)	0.6982 (3)	3.7 (2)
O(4)	1.0933 (6)	-0.0121 (5)	0.8563 (3)	4.9 (2)
C(1)	1.0338 (9)	-0.0303 (6)	0.6169 (4)	3.4 (3)
C(2)	0.742 (1)	-0.1678 (7)	0.5966 (6)	5.4 (4)
C(3)	0.578 (1)	-0.141 (1)	0.5855 (8)	9.3 (6)
C(4)	0.739 (1)	-0.2667 (8)	0.6578 (7)	7.2 (5)
C(5)	0.7239 (8)	0.2993 (5)	0.7201 (5)	3.6 (3)
C(6)	0.722 (1)	0.3802 (7)	0.8679 (6)	4.9 (4)
C(7)	0.829 (1)	0.505 (1)	0.8616 (7)	8.3 (6)
C(8)	0.741 (1)	0.324 (1)	0.9538 (6)	8.0 (5)
C(9)	1.2505 (8)	0.4275 (6)	0.7808 (5)	3.7 (3)
C(10)	1.247 (1)	0.5042 (7)	0.6343 (5)	4.7 (3)
C(11)	1.248 (1)	0.4432 (9)	0.5492 (6)	6.3 (4)
C(12)	1.122 (1)	0.5713 (8)	0.6365 (7)	7.5 (5)
C(13)	0.933 (1)	-0.0571 (6)	0.8772 (5)	4.2 (3)
C(14)	1.218 (1)	-0.0705 (9)	0.8875 (6)	6.5 (5)
C(15)	1.387 (1)	0.033 (1)	0.8933 (9)	10.7 (7)
C(16)	1.203 (2)	-0.172 (1)	0.8253 (8)	9.3 (6)

Table V. Interatomic Distances (Å) and Angles (deg) for $Ge[S_2COMe]_4$ (**1**)

Ge–S(1)	2.200 (2)	S(1)–Ge–S(1)^a	92.4 (1)
S(1)–C(1)	1.702 (8)	S(1)^b–Ge–S(1)^c	92.4 (1)
C(1)–S(2)	1.574 (8)	S(1)–Ge–S(1)^b	118.62 (7)
C(1)–O(1)	1.314 (9)	S(1)–Ge–S(1)^c	118.62 (7)
O(1)–C(2)	1.42 (1)	S(1)^a–Ge–S(1)^b	118.62 (7)
Ge—O(1)	2.945 (5)	S(1)^a–Ge–S(1)^c	118.62 (7)
Ge—S(2)	4.639 (2)	Ge–S(1)–C(1)	105.4 (3)
S(1)—S(1)^a	3.177 (4)	S(1)–C(1)–S(2)	118.9 (5)
S(1)—S(1)^b	3.784 (4)	S(1)–C(1)–O(1)	113.0 (6)
S(1)—S(1)^c	3.784 (4)	S(2)–C(1)–O(1)	128.1 (7)
Ge—S(2)^d	4.854 (3)	C(1)–O(1)–C(2)	119.2 (7)

^{a} $-x, {}^1/_2 - y, z$. ^{b} ${}^1/_4 - y, {}^1/_4 + x, {}^1/_4 - z$. ^{c} $-{}^1/_4 + y, {}^1/_4 - x, {}^1/_4 - z$. ^{d} ${}^3/_4 - y, {}^1/_4 + x, {}^1/_4 + z$.

Table VI. Interatomic Distances (Å) and Angles (deg) for $Ge[S_2COEt]_4 \cdot CS_2$ (**2**)

Ge–S(1)	2.238 (2)	S(1)–Ge–S(1)^a	114.8 (1)
S(1)–C(1)	1.757 (7)	S(1)^b–Ge–S(1)^c	114.8 (1)
C(1)–S(2)	1.613 (7)	S(1)–Ge–S(1)^b	106.88 (5)
C(1)–O(1)	1.324 (7)	S(1)–Ge–S(1)^c	106.88 (5)
O(1)–C(2)	1.462 (8)	S(1)^a–Ge–S(1)^b	106.88 (5)
C(2)–C(3)	1.45 (1)	S(1)^a–Ge–S(1)^c	106.88 (5)
Ge—O(1)	2.932 (4)	Ge–S(1)–C(1)	103.7 (2)
Ge—S(2)	4.725 (3)	S(1)–C(1)–S(2)	120.0 (2)
S(1)—S(1)^a	3.596 (3)	S(1)–C(1)–O(1)	111.6 (5)
S(1)—S(1)^b	3.596 (3)	S(2)–C(1)–O(1)	128.3 (5)
S(1)—S(1)^c	3.771 (4)	C(1)–O(1)–C(2)	119.0 (6)
Ge—S(2)^d	5.297 (3)	O(1)–C(2)–C(3)	107.2 (6)
S(3)–C(4)	1.501 (4)	S(3)–C(4)–S(3)	180.00

^{a} $-x, {}^1/_2, -y, z$. ^{b} ${}^1/_4 - y, {}^1/_4 + x, {}^1/_4 - z$. ^{c} $-{}^1/_4 + y, {}^1/_4 - x, {}^1/_4 - z$. ^{d} ${}^1/_2 + x, y, {}^1/_2 - z$.

extent that they totally decomposed when sent away for analysis and, particularly for the methyl and ethyl derivatives, they decayed rapidly during X-ray data collection to the extent that we were unable to obtain sufficient quality data to solve the structure of $Ge[S_2COEt]_4$ at room temperature. However, sufficient data were collected at room temperature in the case of $Ge[S_2COMe]_4$ to allow the crystal structure to be solved. Surprisingly, the crystal of $Ge[S_2CO(i\text{-}Pr)]_4$ did not decay at room temperature during data collection, and the recent arrival of low-temperature equipment allowed the collection of data at −40 °C on a crystal of $Ge[S_2COEt]_4 \cdot CS_2$ with no decay. The NMR spectra taken immediately after dissolution in carbon disulfide or chloroform

Table VII. Interatomic Distances (Å) and Angles (deg) for $Ge[S_2CO(i\text{-}PR)]_4$ (**3**)

Ge–S(1)	2.231 (2)	O(3)–C(9)	1.303 (8)
Ge–S(3)	2.241 (2)	O(4)–C(13)	1.327 (8)
Ge–S(5)	2.240 (2)	O(1)–C(2)	1.470 (9)
Ge–S(7)	2.237 (2)	O(2)–C(6)	1.502 (8)
S(1)–C(1)	1.742 (7)	O(3)–C(10)	1.480 (8)
S(3)–C(5)	1.744 (7)	O(4)–C(14)	1.484 (8)
S(5)–C(9)	1.752 (7)	C(2)–C(3)	1.51 (1)
S(7)–C(13)	1.761 (7)	C(2)–C(4)	1.50 (1)
S(2)–C(1)	1.615 (7)	C(6)–C(7)	1.45 (1)
S(4)–C(5)	1.647 (7)	C(6)–C(8)	1.50 (1)
S(6)–C(9)	1.638 (7)	C(10)–C(11)	1.48 (1)
S(8)–C(13)	1.603 (7)	C(10)–C(12)	1.51 (1)
O(1)–C(1)	1.345 (7)	C(14)–C(15)	1.53 (1)
O(2)–C(5)	1.299 (8)	C(14)–C(16)	1.48 (1)
Ge–O^a	2.965 (7)	Ge–S^b	4.74 (1)
S–S^c	3.54 (3)	S–S^d	3.87 (2)
S(1)–Ge–S(3)	105.96 (8)	S(1)–C(1)–O(1)	111.9 (5)
S(1)–Ge–S(5)	104.17 (8)	S(3)–C(5)–O(2)	113.9 (5)
S(1)–Ge–S(7)	119.08 (8)	S(5)–C(9)–O(3)	112.7 (5)
S(3)–Ge–S(5)	120.15 (7)	S(7)–C(13)–O(4)	110.2 (5)
S(3)–Ge–S(7)	103.34 (8)	S(2)–C(1)–O(1)	128.1 (5)
S(5)–Ge–S(7)	105.13 (8)	S(4)–C(5)–O(2)	128.6 (5)
Ge–S(1)–C(1)	104.8 (2)	S(6)–C(9)–O(3)	128.8 (6)
Ge–S(3)–C(5)	103.6 (3)	S(8)–C(13)–O(4)	130.0 (6)
Ge–S(5)–C(9)	103.8 (3)	O(1)–C(2)–C(3)	105.0 (7)
Ge–S(7)–C(13)	105.7 (3)	O(1)–C(2)–C(4)	108.9 (7)
C(1)–O(1)–C(2)	119.8 (5)	O(2)–C(6)–C(7)	108.6 (7)
C(5)–O(2)–C(6)	121.3 (5)	O(2)–C(6)–C(8)	103.5 (6)
C(9)–O(3)–C(10)	121.1 (6)	O(3)–C(10)–C(11)	105.7 (6)
C(13)–O(4)–C(14)	119.7 (5)	O(3)–C(10)–C(12)	107.7 (6)
S(1)–C(1)–S(2)	120.0 (4)	O(4)–C(14)–C(15)	103.4 (7)
S(3)–C(5)–S(4)	117.4 (5)	O(4)–C(14)–C(16)	108.0 (8)
S(5)–C(9)–S(6)	118.5 (4)	C(3)–C(2)–C(4)	114.9 (8)
S(7)–C(13)–S(8)	119.7 (5)	C(7)–C(6)–C(8)	115.2 (8)
		C(11)–C(10)–C(12)	115.1 (7)
		C(15)–C(14)–C(16)	116 (1)

^{a} Average of four Ge—O distances. ^{b} Average of four Ge—S distances for S(2), S(4), S(6), and S(8). ^{c} Average of four shorter S—S distances involving S(1), S(3), S(5), and S(7). ^{d} Average of two longer S—S distances involving S(1), S(3), S(5), and S(7).

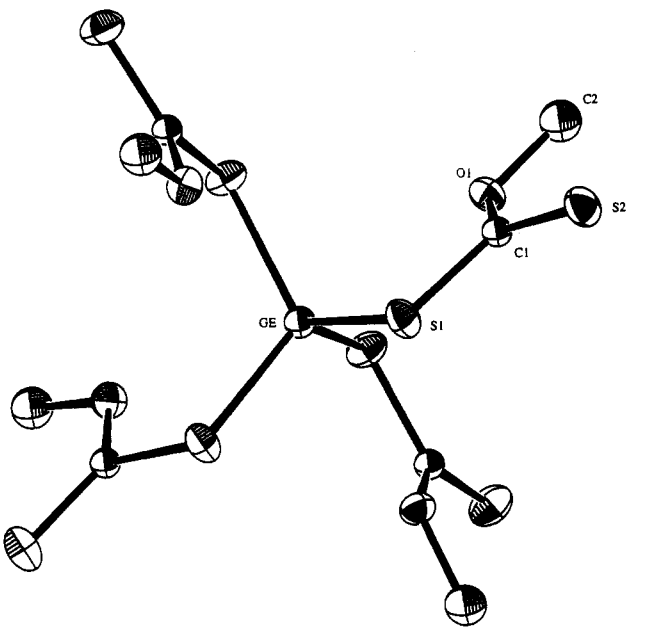

Figure 1. ORTEP plot of the molecule $Ge[S_2OMe]_4$ (**1**). The atoms are drawn with 20% probability ellipsoids. Hydrogen atoms are omitted for clarity.

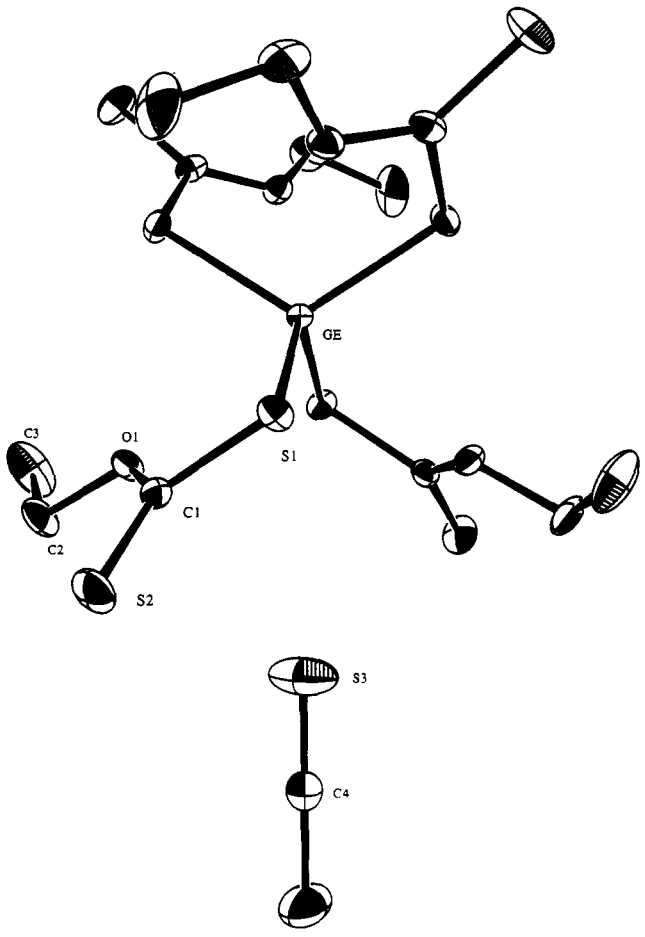

Figure 2. ORTEP plot of the molecule $Ge[S_2COEt]_4 \cdot CS_2$ (**2**). The atoms are drawn with 20% probability ellipsoids. Hydrogen atoms are omitted for clarity.

showed no significant changes over time, suggesting the compounds are reasonably stable in solution.

Attempts were made to prepare the partially substituted chloro derivatives by the introduction of the appropriate stoichiometric amounts of salts to allow for the formation of mono-, bis-, and tris-substituted derivatives in accord with the equations

$$GeCl_4 + KS_2COR \rightarrow Cl_3Ge[S_2COR] + KCl$$

$$GeCl_4 + 2KS_2COR \rightarrow Cl_2Ge[S_2COR]_2 + 2KCl$$

$$GeCl_4 + 3KS_2COR \rightarrow ClGe[S_2COR]_3 + 3KCl$$

In all cases, the ^1H and ^{13}C NMR spectra of solutions before workup showed two characteristic features: a multitude of peaks, suggesting that all three species, at least, were present in all three cases; spectra similar in appearance regardless of the initial ratio of reactants, suggesting that a similar equilibrium position resulted. In no instance was there any success in isolating partially substituted species.

^1H and $^{13}C(^1H)$ NMR Spectra. The ^1H NMR spectrum of the methyl derivative, $Ge[S_2COMe]_4$ (**1**), shows a sharp singlet at 4.13 ppm (Table VIII). This is to be expected if all the xanthate groups are chemically equivalent and hence all linked in a similar manner. The ^1H NMR spectrum of the ethyl derivative, $Ge[S_2COEt]_4$ (**2**), similarly shows one set of peaks with the expected simple first-order splitting, namely, a quartet at 4.60 and a triplet at 1.47 ppm with a coupling constant of 7.15 Hz. Similarly, the ^1H NMR spectrum of $Ge[S_2CO(i\text{-}Pr)]_4$ is first order with a septet due to the –CH group at 5.62 ppm and a doublet at 1.45 ppm with a coupling constant of 6.30 Hz. In all

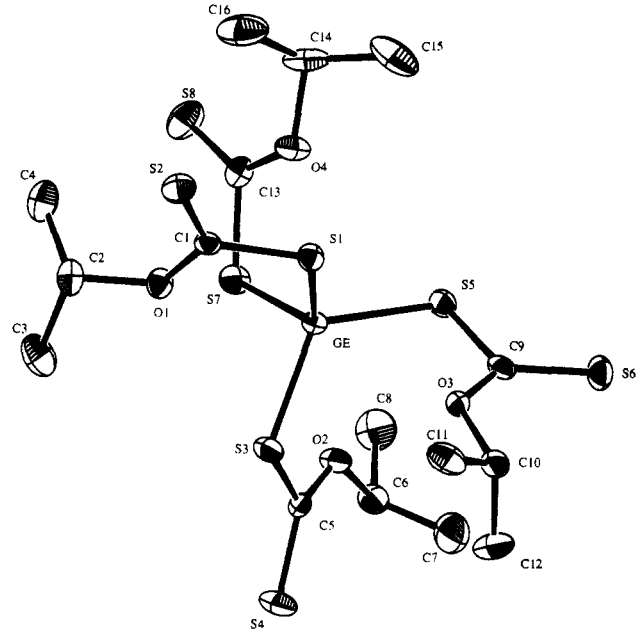

Figure 3. ORTEP plot of the molecule $Ge[S_2CO(i\text{-}Pr)]_4$ (**3**). The atoms are drawn with 20% probability ellipsoids. Hydrogen atoms are omitted for clarity.

cases, the spectra remained constant with changes of temperature. The above data indicate that in each of the three compounds the xanthate groups are both magnetically and chemically equivalent, and so once again identical environments around germanium are to be expected, at least in solution.

In the ^{13}C NMR spectra (Table VIII), all three compounds show a peak due to carbon bonded to oxygen at 61.20, 72.18, and 81.17 ppm, respectively, for the methyl, ethyl, and isopropyl derivative. In the corresponding salts, these shifts are at 60.75, 71.28, and 78.80 ppm so that the changes in shift are very small but in the same direction and similar in all three cases. A peak due to carbon bonded to carbon which is bonded to oxygen is seen at 13.66 ppm for $Ge[S_2COEt]_4$ (**2**) and at 21.13 ppm for $Ge[S_2CO(i\text{-}Pr)]_4$ (**3**). These peaks are shifted by a small and similar amount but in the opposite direction relative to the corresponding peaks in the ethyl and isopropyl salts at 14.67 and 21.59 ppm. The chemical shifts of the dithiocarbonate carbon appear at 207.40, 206.36, and 205.46 ppm in **1**–**3**, respectively, whereas these shifts are at 233.12, 233.71, and 232.82 ppm in the methyl, ethyl, and isopropyl salts. These shifts are larger than the others, presumably reflecting the fact that the environment about the CS_2 carbon is the one most affected by the formation of the Ge–S covalent bond. The similarity of the chemical shifts for all three groups suggests the bonding to germanium should also be similar in all three cases.

Infrared and Raman Spectra. The potassium salts of methyl, ethyl, and isopropyl xanthate used in this study show four strong bands due to the S_2COC group, three that show up as very intense features in the IR spectra in the range 1107–1142 cm^{-1} $(S_2COC)_a$, 1084–1109 cm^{-1} $(S_2COC)_b$, and 1051–1056 cm^{-1} $(S_2COC)_c$ and one as the most intense feature in the Raman effect at 622–666 cm^{-1} $(S_2COC)_d$. The formation of a monodentate linkage and hence one covalent bond to germanium might be expected to lead to decoupling relative to the situation in the symmetrical free anion. As can be seen from the assignments of the tetrakis compounds (Table IX), one band is shifted considerably to higher wavenumber on the formation of the germyl xanthate. Thus, in $Ge[S_2COMe]_4$ (**1**), the intense band in the infrared spectrum at 1245 cm^{-1}, $(S_2COC)_a$, is at considerably higher wavenumber than any possible assignment in the salt. It is also considerably higher

Table VIII. ^1H and ^{13}C NMR Chemical Shifts for Compounds **1–3**[a,b]

no.	compd	$OCH_3/OCH_2/OCH$	CCH_3	$J_{HH'}$, Hz	$OCH_3/OCH_2/OCH$	$OCCH_3$	CS_2
1	$Ge[S_2COMe]_4$	4.13 (12 H, s)			61.20		207.40
2	$Ge[S_2COEt]_4$	4.60 (8 H, q)	1.47 (12 H, t)	7.15	72.18	13.66	206.36
3	$Ge[S_2CO(i\text{-}Pr)]_4$	5.62 (4 H, sept)	1.45 (24 H, d)	6.30	81.17	21.13	205.46

[a] The spectra were recorded in $CDCl_3$ and reported in ppm from Me_4Si. [b] Number of protons and multiplicities are in parentheses (s = singlet, d = doublet, t = triplet, q = quartet, sept = septet).

Table IX. Selected Features and Their Assignments in the Vibrational Spectra of Compounds **(1–3)**[a,b]

$Ge[S_2COMe]_4$ (1)		$Ge[S_2COEt]_4$ (2)		$Ge[S_2CO(i\text{-}Pr)]_4$ (3)		
IR[c]	Raman[d]	IR[c]	Raman[d]	IR[c]	Raman[d]	assgnt
1245 (s)	n.o.[e]	1246 (s, br)	n.o.	1250 (s)	n.o.	$\nu(S_2COC)_a$
1051 (s)	1053 (20)	1033 (vs)	1038 (90)	1021 (vs)	1022 (66)	$\nu(S_2COC)_b$
883 (s, br)	n.o.	882 (s, br)	n.o.	891 (s, br)	n.o.	$\nu(S_2COC)_c$
640 (vw)	653 (62)	n.o.	651 (36)	692 (vw)	695 (39)	$\nu(S_2COC)_d$
450 (vw)	443 (30)	420 (vw)	423 (100)	429 (vw)	430 (50)	$\nu(Ge\text{–}S)_{asym}$
400	391 (81)	347 (vw)	353 (74)	374 (vw)	365 (100)	$\nu(Ge\text{–}S)^{sym}$
	203 (100)	n.o.	181 (77)	n.o.	174 (77)	$\delta(Ge\text{–}S)_{asym}$
	136 (19)	n.o.	144 (10)	n.o.	146 (3)	$\delta(Ge\text{–}S)_{sym}$

[a] Parentheses denote relative intensities in the Raman effect. [b] s = strong, w = weak, v = very, br = broad. [c] Run as CsI pellets. [d] Run as a solid in a glass capillary. [e] n.o. = not observed.

than the higher component in CS_3^{2-} which is at 940 cm^{-1},[13] and so may well predominantly arise from the S_2C–O stretch, suggesting that this CO bond should be somewhat longer than in CO_3^{2-} but considerably shorter than in dimethyl ether. This $(S_2COC)_a$ band is seen at essentially the same position in the spectra of the ethyl and isopropyl analogues. The second band in the spectrum of $Ge[S_2COMe]_4$ is seen at 1051 cm^{-1}. The question arises as to whether this represents a small shift in $(S_2COC)_b$ from 1083 cm^{-1} in the salt or arises from the vibration that was previously described as $(S_2COC)_c$ in the salt in the same region of the spectrum. The latter seems likely and should correspond to the O–CH_3 stretch because this motion is least coupled in the free ion and so should not change on formation of the germanium–sulfur bond. The position at 1051 cm^{-1} is also close to the average value in dimethyl ether,[14] suggesting an O–CH_3 bond of approximately 1.42 Å. Similar arguments can be made for the major origin of the bands assigned as $(S_2COC)_b$ in the ethyl and isopropyl analogues, although the band appears to shift a small but increasing amount from the ethyl to the isopropyl compound, suggesting that the O–CH bonds might be longer in **2** and **3**. The third intense band in the infrared spectrum in the 882–891-cm^{-1} region, $(S_2COC)_c$, should then result primarily from the stretching of the terminal C–S bond. The intensity suggests a motion resulting in a significant change in dipole moment, as would be the case for a S_2COC group fixed at one end by a single bond to germanium. If this motion is uncoupled then the value of ca. 880 cm^{-1} is greater than the weighted average in the CS_3^{2-} ion of 800 cm^{-1}, suggesting a C–S bond shorter than but similar to that found in the CS_3^{2-} anion of 1.71 Å.[15] The $(S_2COC)_c$ vibration appears in essentially the same position in the ethyl and isopropyl analogues. The fourth band, which is Raman active, shifts to higher wavenumber in $Ge[S_2COMe]_4$ at 653 cm^{-1} relative to its position in the salt at 622 cm^{-1}, but at the same time it loses intensity relative to other features in the Raman spectrum. This is to be expected if, as a result of the formation of the Ge–S bond, this motion now more accurately reflects the stretching of an isolated C–S single bond. The $(S_2COC)_d$ vibration is in a similar position in the ethyl analogue, but in $Ge[S_2CO(i\text{-}Pr)]_4$ it is seen at 695 cm^{-1} compared to 662 cm^{-1} in the salt, although this represents a similar shift of ca. 30 cm^{-1}. In a study involving force constant calculations on compounds containing a single Ge–S(C) bond, the stretching vibration ν(C–S) was found consistently at approximately 700 cm^{-1} and the force constant contributions indicated an essentially pure C–S stretch with no interactions.[16]

In the same study, the Ge–S stretching vibration was consistently observed at approximately 400 cm^{-1} and the Ge–S asymmetric and symmetric stretching modes are both strongly active in the Raman effect in $Ge[S_2POMe_2]_4$,[17] where they are assigned at 387 and 363 cm^{-1}, respectively. The same phenomena are observed for all the $Ge[S_2COR]_4$ species, but the weighted average of the Ge–S stretches is considerably higher in $Ge[S_2COMe]_4$, suggesting a stronger Ge–S bond. The Ge–S asymmetric and symmetric deformation modes are higher for the xanthates than the corresponding modes in the dithiophosphate, suggesting a "stiffer" framework in the xanthates consistent with its delocalized π-bond nature.

Molecular Structures of $Ge[S_2COMe]_4$ (1), $Ge[S_2COEt]_4 \cdot CS_2$ (2), and $Ge[S_2CO(i\text{-}Pr)]_4$ (3). Tetrakis(*O*-methyl dithiocarbamato)germanium(IV) (**1**) crystallizes in the relatively unusual, highly symmetrical space group $I4_1/a$. Thus, all four Ge–S bonds are identical and the bond length of 2.200 (2) Å is the shortest of those reported to date for this type of ligand and clearly may be considered a strong bond when the length is compared to the sum of the covalent radii of germanium and sulfur of 2.26 Å.[18] The ORTEP diagram of $Ge[S_2COMe]_4$ is given in Figure 1. The four S atoms attached to germanium in **1** lead to two angles of 92.4 (1)° and four of 118.62 (7)°. Also, the xanthate groups whose S atoms subtend 92.4 (1)° angles are essentially coplanar with each other and have angles close to 90° relative to the other two xanthate groups. The immediate coordination about germanium may be considered a tetrahedral arrangement distorted along the 2-fold axis bisecting the 92.4 (1)° angles. However, if the four oxygen atoms at 2.945 (5) Å are included in the coordination sphere, then the environment around germanium is eight-coordinated in a distorted-cubic arrangement. Tetrakis(*O*-ethyl dithiocarbonato)germanium(IV) (**2**) also crystallizes in $I4_1/a$, but in this case a molecule of CS_2 is also trapped in the crystal, as can be seen in the ORTEP diagram in Figure 2. The Ge–S bond of 2.238 (2) Å is not as short as in **1**, and the distortion from all tetrahedral angles is much less and is such as to give four S–Ge–S angles of 106.88 (5)° and two of 114.8 (1)°.

Although tetrakis(*O*-isopropyl dithiocarbonato)germanium(IV) (**3**), crystallizes as $P\bar{1}$, the environment around germanium is still such as to give four Ge–S bonds that are very similar although

(13) Ross, S. D. *Inorganic IR and Raman Spectra*; McGraw Hill, London, 1972; p 160.
(14) Kanazawa, Y.; Nukada, K. *Bull. Chem. Soc. Jpn.* **1962**, *35*, 612.
(15) Philipot, E.; Lindquist, O. *Acta Crystallogr.* **1970**, *B26*, 877.
(16) Drake, J. E.; Henderson, H. E.; Khasrou, L. N. *Spectrochim. Acta* **1982**, *38A*, 31.
(17) Chadha, R. K.; Drake, J. E.; Sarkar, A. B. *Inorg. Chem.* **1987**, *26*, 2885.
(18) Wells, A. F. *Structural Inorganic Chemistry*, 4th ed.; Clarendon Press: Oxford, England, 1975; p 236.

all are longer than in **1** and close to the value in **2**, ranging from 2.231 (2) to 2.241 (2) Å. The ORTEP diagram of $Ge[S_2CO(i\text{-}Pr)]_4$ is given in Figure 3. Like **2**, but unlike **1**, the Ge–S bonds subtend four angles that are less than the tetrahedral angle ranging from 103.34 (8) to 105.96 (8)° and two angles that are greater at 119.08 (8) and 120.15 (7)°. Thus, the overall distortion from a perfect tetrahedral arrangement is again less than that found in the methyl analogue **1** but is in the opposite sense. The distortions in **1** and **3** are larger than were observed for the related phenyl derivatives, $Ph_2Ge[S_2COMe]_2$ and $Ph_2Ge[S_2CO(i\text{-}Pr)]_2$,[1,2] which suggests that these xanthate groups may have a significant role in determining the stereochemistry. The Ge–S distance of 2.200 (2) Å in **1**, 2.238 (2) Å in **2**, and the average of 2.237 (4) Å found in **3** are all shorter than the 2.272 (2) Å in $Ph_3Ge[S_2CO(i\text{-}Pr)]$, 2.254 (3) and 2.262 (3) Å in $Ph_2Ge[S_2COMe]_2$, and 2.252 (3) Å in $Ph_2Ge[S_2CO(i\text{-}Pr)]_2$.[2] This type of shortening of the bond is expected as the more electronegative group replaces the less electronegative one, which in this case is the phenyl group. The same type of behavior was observed in the analogous germanium dithiophosphate series.[17,19,20]

Clearly, in **1–3** all of the xanthate groups are monodentate, giving a total of four germanium–sulfur bonds in each case. The xanthate group is oriented so that the oxygen atom, rather than the second sulfur atom, is in closer proximity to the germanium, with Ge- - -O distances of 2.945 (4) Å in **1**, 2.932 (4) Å in **2**, and an average of 2.965 (7) Å in **3**. The distances are closer to the sum of the van der Waals radii of germanium and oxygen (3.40 Å) than to the sum of the covalent radii (1.96 Å) and so are probably too long to allow oxygen to play a significant role in the coordination sphere about germanium. The lower symmetry in the isopropyl xanthate is emphasized by the fact that no two xanthate groups are close to coplanar, as is the case for the other two derivatives. The nonbonding Ge- - -S distances of 4.639 (2) Å for **1**, 4.725 (3) Å for **2**, and an average of 4.74 (1) Å for **3** are comparable to those found in the phenylgermanium xanthates.[1,2]

The C—SGe and C=S distances clearly correspond to a long and short bond in all three compounds. Despite the fact that the C—S bonds are of different length, the S(1)—C(1)—S(2) angle remains close to 120°. It was inferred from the vibrational spectra that the terminal C=S bond might be approaching a true double bond in all three compounds, and it is indeed comparable to the C=S bond length of 1.5 Å in OCS, particularly in **1**. Also, it was suggested that the C—SGe bond might now be closer to a true single bond, particularly in **3**, and the average value of 1.746 (9) Å is considerably longer than the 1.71 Å reported for CS_2^{2-}.

The S(2)—C—O(1) angle is by far the one most opened up from 120°, to 128.1 (7)° in **1**, 128.3 (5)° in **2**, and an average of 128.9 (8)° in **3** for the four groups. This is consistent with the delocalized π-system now becoming shared more between the terminal C=S and S_2C—O bond and with the large shift of $(S_2COC)_a$ to 1245 cm^{-1}, indicating a relatively short S_2C—O bond, as is the case: 1.314 (9) Å in **1**, 1.324 (7) Å in **2**, and an average of 1.30 (5) Å in **3**. The similarity of the bond lengths appears to confirm the supposition based on the similarity of the positions of the vibrational mode. It was also suggested that the band assigned at 1051, 1033, and 1021 cm^{-1} for **1–3** was indicative of an O—CR_3 bond, $R_3 = H_3$, $H_2(CH_3)$, $H(CH_3)_2$, that was essentially a single bond. This is confirmed by the X-ray structure which gives an O—CH_3 bond of 1.42 (1) Å in **1**, 1.462 (8) Å for O—CH_2 in **2**, and an average value for the O—$CH(CH_3)_2$ bond of 1.48 (1) Å in **3**, the longer bond in the latter case being consistent with the considerable shift of the vibrational frequency to lower wavenumber. However, in general, the xanthate groups are similar in all three compounds, which is what was deduced from the NMR spectra.

Within the methyl analogue, **1**, the distortion from all tetrahedral angles leads to relatively short S(1)–S(1) distances of 3.177 (4) Å between the S atoms attached to germanium that subtend the 92.4 (1)° angle and, of course, much longer distances of 3.784 (4) Å for the other two contacts. By contrast, in the ethyl (**2**) and isopropyl (**3**) analogues, where the distortion is of a different nature and less dramatic, the closest S–S contacts of this type are 3.596 (3) Å for **2** and an average of 3.513 (3) Å for **3**. Nonbonding distances, both inter- and intramolecular, were examined for any evidence of unusually short distances that might be indicative of secondary interactions and hence of the mode of decomposition. The closest intermolecular distance between a germanium atom and any sulfur atom of an adjacent molecule in **1** is 4.854 (3) Å, which is slightly longer than the distance to the nonbonding S atom within the molecule of 4.639 (2) Å. Thus, there is no indication of a bridge involving sulfur atoms. Corresponding Ge–S nonbonding intermolecular distances in the isopropyl analogue range from 4.761 (3) to 4.985 (3) Å. In **2**, which decomposed too rapidly at room temperature to allow X-ray data collection, the closest corresponding Ge- - -S distance is 5.297 (3) Å, suggesting the decay is not intermolecular. There are no close contacts involving oxygen and the nearest Ge–Ge intermolecular distance is 6.659 (1) in **1** and much longer in **2** and **3** at 7.956 (3) and 8.366 (1) Å, respectively. This seems to confirm that the molecules are simply packed together with no intermolecular interactions of significance. Thus, the nonbonding distances, both intra- and intermolecular, do not give any evidence of likely modes of decomposition, despite the fact that all three compounds decayed even when sealed in a capillary tube.

Acknowledgment. We wish to thank the Natural Sciences and Engineering Research Council of Canada and Imperial Oil Canada for financial support (J.E.D.) and the University of Windsor for a bursary (A.G.M.).

Supplementary Material Available: Tables S1–SVII, listing experimental details, anisotropic thermal parameters for non-hydrogen atoms, and final fractional coordinates and thermal parameters for hydrogen atoms (5 pages). Ordering information is given on any current masthead page. Structure factor tables may be obtained directly from the authors.

(19) Chadha, R. K.; Drake, J. E.; Sarkar, A. B. *Inorg. Chem.* **1985**, *24*, 3156.
(20) Chadha, R. K.; Drake, J. E.; Sarkar, A. B. *J. Organomet. Chem.* **1987**, *323*, 271.